UNIVERSITÀ DEGLI STUDI DI PADOVA

DIPARTIMENTO DI INGEGNERIA

DIPARTIMENTO DI INGEGNERIA DELL'INFORMAZIONE

CORSO DI LAUREA IN INGEGNERIA BIOMEDICA

"TRUNK MUSCLE ACTIVATION AND COACTIVATION CHANGES IN PATIENTS WITH MULTUPLUS MYELOMA UNDERGOING VERTEBRAL CONSOLIDATION SURGERY: A STUDY PERFORMED BY USING MOVEMENT ANALISYS TECNOLOGIES"

Relatore: Prof.ssa Sawacha Zimi

Laureanda: Zampa Benedetta

Correlatore: Ing. Ranavolo Alberto

ANNO ACCADEMICO 2022 – 2023

Data di laurea 13.03.2023

INDEX

1. Introduction

Multiple myeloma (MM) is a neoplasm characterized by the clonal proliferation of malignant plasma cells. Plasma cell disorders constitute a group of blood diseases characterised by the presence of monoclonal plasma cells in the medullary space or, less commonly, in other tissues. In people suffering from MM, plasma cells expand at the level of the bone marrow, causing the typical multiple osteolytic lesions. As a result, the spinal column is the bone site that is most frequently affected by lesions associated with MM. Bone localizations of disease and the subsequent possible vertebral collapse can result in spinal cord or radicular compression with subsequent neurological signs and symptoms (Marjanović S et al., 2012, Tosi P 2013). The main symptomatology experienced by patients with MM includes kidney damage, bone pain, anaemia-related asthenia and infections (Anderson KC et al., 2021).

MM accounts for 1-2% of all neoplasms and 10% of haematological malignancies and predominantly affects the elderly: 38% of patients are older than 70 years, while only 10% are younger than 50 years (Castillo JJ, 2016). The age-adjusted incidence rate of MM ranges from 2.5 to 7.2 per 100,000 in Western countries (Kristinsson SY et al, 2003). The AIOM (Associazione Italiana di Oncologia Medica), in its 2017 guidelines, indicates that in Italy such incidence is 8.1 new cases per 100,000 inhabitants each year in the female population (representing 1.3% of all cancers) and 9.5 in the male population (1.2% of all cancers).

Patients with multiple spinal injuries often complain of pain and stiffness that limit motility and activities of daily and work life, notably, in 70% of cases, bone pain is the first symptom reported when the disease begins (Tosi P 2013).

The most common clinical feature in patients with MM is back pain, mainly due to: spinal cord entrapment; neural irritation; and local inflammation. Depending on the location of the vertebral compression, different motor deficits may occur: lumbar compression results in sensory loss with radicular pain, whereas symmetrical lower limb weakness with back pain is more typical of thoracic compression (Chen B et al., 2021).

The second major symptom of spinal cord compression[1] (SCC) is motor dysfunction, which manifests as weakness in the lower limbs (Chen B et al.,2021). SCC is found in patients with MM with an incidence of 7.8% (Sharma A et al., 2017, Wickstroem LA et al., 2020, Chen B et al., 2021). Another important aspect to consider in MM is chemotherapy-induced quality of life (QoL) (Argyriou AA et al., 2008, Shaheen NA et al.,2020). Scientific evidence shows that both bone weakness and the onset of neuropathy contribute to making it difficult for patients to perform basic activities such as walking, climbing stairs or getting up from a chair (Tosi P 2013, Shaheen NA et al.,2020). Various sensory symptoms such as paraesthesia, tingling or numbness are added to these disabilities (Tosi P 2013). Symptom burden affects physical function and physical activity levels, which may put people at risk of physical decline (Larsen RF et al.,2020).

Furthermore, it is evident that the destruction of bone seen in people affected by multiple myeloma is a leading cause of morbidity and mortality (Larsen RF et al., 2020).

With all the symptomatology we have just seen, MM turns out to be a very debilitating disease that reduces the quality of life of its sufferers (Croucher PI et al., 1998, Tosi P 2013, Shaheen NA et al., 2020).

Given the complexity of the clinical picture, patients need personalised care. In order to identify the best treatment, we first have to objectively quantify the problems afflicting the patient; this is possible by means of a three-dimensional reconstruction of movement; an analysis of muscular behaviour and the set of shear and compressive forces experienced by the various joint groups.

Human movement analysis is an important branch of bioengineering research due to its vital relevance to clinical applications. Indeed, its implementation can provide qualitative and quantitative characterisation of comparisons between normal and pathological movements, as well as the evaluation of treatment protocols (Wong WY et al., 2007). Movement analysis is a combination of three disciplines for the description of motion: kinematics, kinetics and surface electromyography (sEMG) (Sandrini S et al., 2020). Kinematic analysis is a description of the movement of a

[1] Spinal cord compression is an important complication of multiple myeloma and has the potential to cause loss of neurological function.

body in space and involves the study of instantaneous angular positions in the following planes: sagittal (flexion-extension), frontal (abdo-adduction) and transverse (intra-extra rotation). Furthermore, it may provide information on linear and angular displacements, velocities and accelerations of body segments and joints.

The kinematics of the movement can be determined with the aid of technologies such as opto-electronic systems (Sandrini S et al., 2020). As a matter of fact, opto-electrical analysis allows the position of joints and body segments to be measured and through the opto-electrical detection unit, the orientation of body segments is derived by processing the data reduction (Wong WY et al., 2007).

Kinetics (or dynamics) is the discipline of physics concerned with the study of forces that alter the state of motion of a body. It provides information concerning the force interactions between the subject and the ground and allows the development of internal moments in individual joints to be deduced. Other information that can be obtained includes joint shear and compression forces, angular momentum, support moments, joint powers and global stiffness.

Surface electromyography records the electrical signal that causes skeletal muscles to contract. This signal is detected by probes placed on the surface of the skin. It permits the extrapolation of simple information about activation intervals to more complex information such as neural control strategies (Sandrini S et al., 2020).

The literature shows that physical activity produces great improvements in counteracting the progression of motor deficits (Larsen RF et al., 2020). It is therefore essential not only to design an ad hoc rehabilitation pathway, but also to monitor the effects and effectiveness of such treatment.

Although it will not be the subject of this thesis, the tools we have used to evaluate the effects of vertebroplasty will find further application in monitoring the progress of rehabilitation treatments.

A pathological fracture of the spinal bone is associated with a sudden and abrupt increase in pain perceived by the patient (Chen B et al., 2021). Other critical consequences of spinal injuries vertebral collapses are kyphosis, walking difficulties, deformities and permanent disability or paralysis (Tosi P 2013).

Vertebral collapses may benefit from biomechanical stabilization of microfractures by vertebroplasty, both to control pain and to prevent further damage to the spine.

The main types of vertebroplasty that are performed are:

- Percutaneous vertebroplasty, it is an interventional radiology procedure by which pathological vertebral fractures are treated by injecting a biocompatible "cement" into the body of the vertebra.

- Balloon kyphoplasty, which involves "dilating" the fractured vertebra with a balloon before the cement is injected. This dilation allows the natural height of the collapsed vertebra to be restored.

The current scientific scenario supports the positive effects of vertebroplasty on patients' lives. As a matter of fact, the literature shows that such a procedure provides patients with important and lasting pain relief (McDonald RJ et al. 2008, Chen LH et al. 2012).

Assuming that vertebroplasty benefits the patient, means to hypothesize that muscle coactivations and stiffness, will decrease after the surgery. Indeed, the literature describes increased joint stiffness as one of the main consequences of agonist-antagonist muscle co-activation (Lee PJ et al., 2006, Latash ML, 2018).

Muscle coactivation refers to the simultaneous contraction of a muscle (or muscle group) and its antagonist (Ranavolo A et al., 2021). This phenomenon is aimed with the purpose of motor control, modulating joint stiffness and occurs when there is a need to stabilize a joint (Latash ML, 2018, Ranavolo A et al., 2021). Thus, the central nervous system (CNS) can take advantage of coactivation for various reasons: protecting the joint, performing precision tasks, implementing "fear-avoidence" behaviour, and inexperience. Excessive coactivation can be harmful, hindering the articulatory moment necessary for the execution of the motor task. CNS abuse of coactivation results in increased metabolic cost with reduced net momentum and power generated (Varrecchia T et al. 2018). Increased joint compressive and shear forces are also observed, which can lead to cartilage loss. In the district of interest in this study, the trunk, there is significant coactivation during the lifting task, with the purpose of stabilizing the spine (Lee PJ et al., 2006). But as mentioned earlier, high coactivation, results in increased compression and shear forces, in this case on the lumbosacral joint (L5-S1) (Ranavolo A et al., 2021).

1.1. Aim of the thesis

This study aims to test the above hypothesis and to objectify how spinal motility and stability vary after vertebroplasty surgery.

The application of movement analysis, in this study, is pivotal for the assessment of:

- stiffness of the upper body district;
- stress fore affecting the L5-S1 joints of the spine;
- behaviour of various joint districts;

1.2. Outline

The first chapter of this thesis, "Materials and Methods", presents the tools used in the study and the methodologies for data collection, processing and analysis. The chapter also defines the study population and describes the parameters derived from the data analysis from a statistical point of view.

In the "Results" section, the results of the study carried out are presented in histogram form. In the same section, the results of the statistical tests applied are also presented in tabular form.

The "Discussion" section is devoted to commenting on the results obtained.

Finally, a reflection on the limitations of the study will be made in "Limitations", the last paragraph of this thesis.

2. Materials and Methods

2.1. Setting

The acquisition of the data and parameters necessary for the study was collected at the Multifactor Analysis Laboratory of the Oncology Reference Centre (CRO) in Aviano, Pordenone. The ethical aspects of this clinical trial follow the guidelines of the Declaration of Helsinki and all participants signed an informed consent form after receiving a full explanation of the study procedure. The study was approved by the local ethics committee: CEUR-FVG (Single Regional Ethics Committee) under approval number: CRO-2020-35.

2.2. Study population

All patients with multiple myeloma and candidates for vertebroplasty who meet the following eligibility criteria will enter the study.

Inclusion criteria:

- Age ≥ 18 years old;
- Historically confirmed diagnosis of MM and with multiple vertebral lesions;
- Clinical indication and eligibility to perform vertebroplasty procedure;
- Performance Status (ECOG) 0-2;
- Life expectancy greater than three months at the time of enrolment;
- TC skeleton in its entirety low resolution at disease onset and/or follow-up;
- Spine pain with stiffness and functional impediment pre vertebroplasty;
- Able to express appropriate consent to participation.

Exclusion criteria:

- Spinal cord compressions;
- Unstable vertebral injuries, requiring orthopaedic bracing;
- Risk of spinal cord injury;
- Body mass index (BMI) > 28kg/sqm;
- Absence of signed infirm consent form.

2.3. Biomechanical parameters acquisition:

Data acquisition is carried out through three acquisition systems:

- Optoelectronic system (SMART-DX 60000, BTS, Milan, Italy):
  Consisting of 5 infrared cameras (340Hz sampling rate) for detecting passive spherical markers
- 1 Force plate (P 6000, BTS, Milan, Italy):
  The platform is embedded in a wooden walkway (680Hz sampling rate)
- Wi-Fi transmission surface electromyography system (FreeEMG 1000 System, BTS, Milan, Italy) consisting of 8 probes, 4 of which are waterproof.

These systems will allow us to define the kinematics, kinetics and sEMG data of the movement, respectively.

Kinematic analysis of human movement allows us to three-dimensionally reconstruct the movements of each joint in space. With this data, we can reconstruct the range of motion of various joint groups. The cameras emit a beam of infrared light that invests passive spherical markers placed on specific prominent bony landmarks points. The markers are coated with an aluminium powder that reflects the infrared beam; this enables the optoelectronic system to measure the three-dimensional coordinates of the markers themselves.

The positioning of the markers has been performed by following the Davis Modified Protocol, which allows the reconstruction of lower limb, upper limb and torso movement. The Davis protocol involves an initial phase of anthropometric data gathering of the patient, such as: height, weight, length of the subject's tibia, distance between the femoral condyles or knee diameter, distance between the malleoli or ankle diameter, distance between the anterior iliac crests, and pelvic thickness.
In a successive step, the twenty-four retro-reflective markers were placed on the following repere points: the 7th cervical vertebra (c7) and sacrum, both right and left: acromion, olecranon, ulnar styloid process, radius styloid process anterior superior iliac spine, greater trochanter, lateral femoral condyle, head of the fibula, lateral malleoli, head of the metatarsal, and heel. Four additional stick markers were placed at one third of the length of the femur and leg, as shown in figure1 (Taratelli A et al. 2020). The kinematic analysis of movement is essential in order to allow us to contextualise the information extrapolated from the kinetic analysis and the surface electromyography. Thanks to the above-mentioned features, it is possible to identify the portion of the skin where the best quality and most stable signal can be obtained.

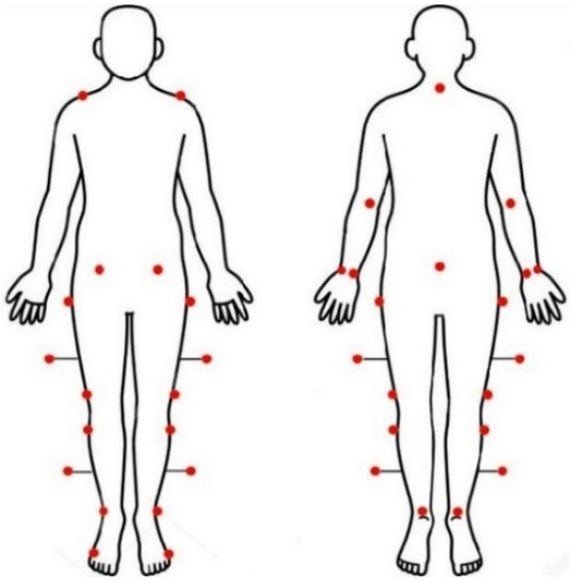

Figure 1 Position of markers in the Modified Davis protocol used during data acquisition.

The force platform allows us to measure: vectorial forces exchanged with the ground in three axes. From these data we can reconstruct the stress forces and moments acting on the various joints. For this reason, force platforms are applied in several fields, such as: diagnostics, rehabilitation and the study of postures.

The surface electromyography system records the sEMG signal generated by the electrical stimulus that induces the convergence of actin and myosin fibres, resulting in muscle contraction.

With the aim of studying trunk behaviour, the muscular activities that were investigated came from two antagonistic muscle groups: the erector spinae longissimus (ES), an extensor, and the rectus abdominis superior (RAS), a flexor. To record the myoelectric signal, once the skin has been adequately prepared, we proceed with the placement of the surface electrodes (2 cm in diameter; H124SG Kendall ARBO, Tyco Healthcare, Neustandt/Donau, Germana) on which the sensors will be placed. Since the main source of noise in sEMG recordings is electrode noise, the electrode-gel skin impedance (ZEGS) has the ability to significantly affect the quality of the detected signal. ZEGS is therefore the limiting factor in the detection of very small potentials. As ZEGS is mainly due to the gel-skin contact, it is recommended that the area of skin on which the sEMG signal is to be recorded is treated before the electrodes are applied (Merletti R et al., 2004, Merletti R et al., 2016). In order to ensure good skin-electrode contact and low electrode–skin impedance, pre-gelled Ag/AgCl electrodes were used in accordance with the "European

Recommendation for Surface Electromyography" (Hermens HJ et al. 2000). Keeping with the guidelines drafted by SENIAM (surface EMG for a non-invasive assessment of muscles), we place the sEMG electrodes with the orientation[2] parallel to the muscle fibres. The main factors that significantly affect the stability of a sEMG recording are: the presence of other active muscles in the vicinity of the SEMG sensor (crosstalk) and the presence of motor points and/or tendons. Indeed two further important carefulness are: (1) to position the sEMG probe away from the edges with other muscles and midway between the distal motor endplate zone and the distal tendon; (2) to place the two electrodes at the recommended inter-electrode distance[3] (that is 20 mm or less than a quarter of the muscle fibre length for short muscles). This makes the acquisitions more stable (minimising tendon and motor plate effects) and provides a good compromise between the need to limit spectral changes and the need to improve signal amplitude and signal-to-noise ratio. (Hermens HJ et al. 2000, Merletti R et al.,2004).
As mentioned above, the purpose of this study is to assess how vertebroplasty affects patients' everyday life. For this purpose, patients were asked to perform three simple tasks:

- Lifting: during this task, patients were instructed to lift a light weight [4], placed at an initial height of approximately 50 cm, to the level of their torso and then return it to the initial position. This allowed us to extrapolate the corresponding lowering task from the data. The suitability of this task in the study is related to the fact that lifting is a manual material handling activity and is associated with both lower back pain and lower back injuries (Varrecchia T et al. 2022).

- Sit to stand: the scientific background states that the ability to sit and stand is impaired by many common pathologies, including lower back pain. The evaluation of the benefits of vertebroplasty on the ability to perform this activity is due to the fact that this movement has a great impact on the patient's

[2] Orientation is defined as the position of the line between the two electrodes in relation to the direction of the muscle fibres.

[3] Inter-electrode distance (IED) is defined as the centre-to-centre distance between the conductive areas of two electrodes in the bipolar configuration.

[4] Light weight is defined as an object that weighs no more than 3 kg.

independence and quality of life. Both sitting and standing require strength, coordination, balance and flexibility (Norman-Gerum V et al. 2020).

For the sit-to-stand test, the patient starts sitting with the legs outside the force plate, when the recording starts the patient can place the feet inside the force plate and stand up, he stands for a few seconds after which he can sit down again.

- Stand to sit: the considerations made for sit-to-stand can also be applied to sitting. With regard to the execution of the stand-to-sit task, the patient starts the task in a standing position outside the platform, then, once the acquisition has started, approaches the chair and sits down, maintains this position for a few seconds and then stands up again. It is important that the patient is not on the force platform before the start of the acquisition, otherwise the dynamometric system will calibrate to the perceived weight, failing to measure the change in weight force generated by the patient. This shrewdness should also be extended to the lifting task.

- Walking: the study of human gait (gait analysis) provides important biomechanical information about a patient's health status, allowing the impact of disease on gait to be assessed (Serrao M, et al., 2017). Although gait assessment can provide valuable information on the effect of vertebroplasty, thereby improving the understanding of pathogenesis and indicating the most suitable therapeutic strategy, the data collected from gait task analysis will not be presented in this thesis.

Only after the initial calibration procedure of the laboratory, the first data acquisition of the above tasks was carried out.

2.4. Data Analysis

Data analysis was performed using BTS's SMART package (SMARTanalyzer and SMARTtracker), MATLAB (Version: 9.10.0.2015706 (R2021a)) and Excel.

An initial phase of analysis consisted of the three-dimensional reconstruction of the movement during the motor tasks, which was carried out using the SMARTtracker

programme by first constructing a model for each task and then applying the corresponding model to each trial. In this analysis phase, the software synchronises the data gathered by the force platform, the optoelectronic cameras and the surface electromyography probes (Ranavolo A et al., 2015).

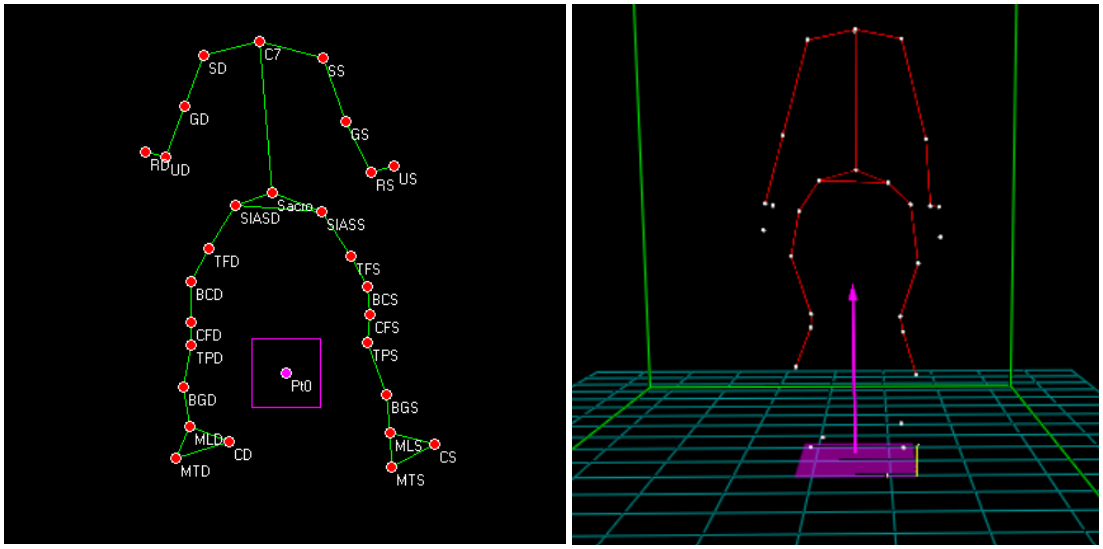

Figure 2: On the left you can see the reconstruction with SMARTtracker of the segments between the different reference points and the pt0 vector of the platform. On the right is the actual reconstruction of the patient's movement with SMARTanalyzer.

The movement reconstruction allowed us to define four instants of time: “Start”, “Intermediate1”, “Intermediate2” and “Stop”, identifying them from the movement trajectories of specific markers during the task, as can be seen in Figure 3. Thanks to these temporal instants we were able to describe a time interval over which to normalise the electrical signals. In the lifting task, the “Start” corresponds to the moment when the person bends over the object, the “Intermediate1” to the moment when the patient stands with the weight at torso height, “Intermediate2” to the moment when the person starts lowering the weight and the “Stop” to the moment when the patient returns the object to its initial position. We can divide this test into lifting (from start to intermediate) and lowering (from intermediate to stop). In the temporal definition of the sit-to-stand motor task, the 'start' moment coincides with the person sitting in the chair, the 'intermediate1' moment with the patient standing, the 'intermediate2' when the subject is about to sit and the “Stop” with the person sitting again. Conversely, the “stand to sit” test recognises as the “Start” the patient standing

in front of the chair, the “Intermediate1” the patient sitting, the “Intermediate2” as soon as the person is in the process of getting up and the “Stop” the patient standing again. This allows us to extrapolate sit to stand from stand to sit and vice versa. It is important to identify two intermediate moments so that any moments where the patient statically maintains the position are not considered part of the task. If such moments were included, the sEMG results would be distorted.

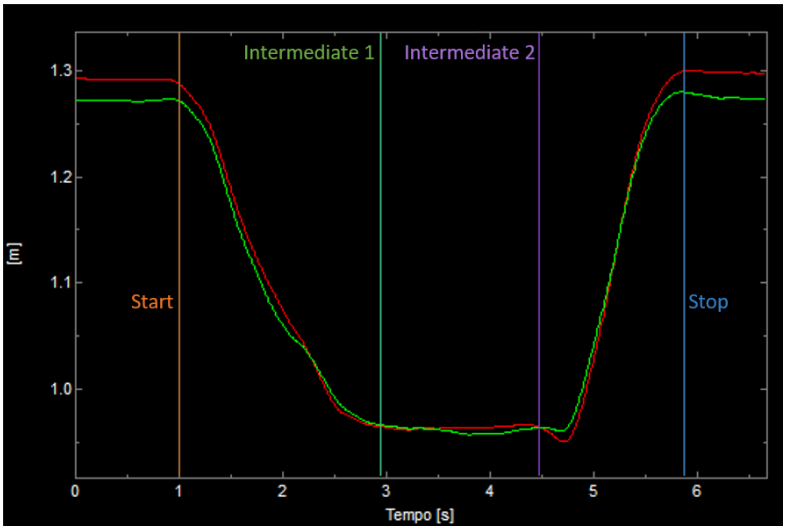

Figure 3: Example of the selection of the instants 'Start', 'Intermediate 1', 'Intermediate 2' and 'Stop' in the 'stand to sit' task. The curves show the reconstruction of the change in height (y-axis) of the markers positioned on the left and right shoulders.

The SMART Analyser software was used to process the sEMG data and reconstruct the trend of the flexion-extension angle of the trunk during the performance of the task. The range of motion (RoM) of the trunk was calculated from this data. The SMARTanalyzer was also used to process the sEMG signals.

The electromyographic signal recorded by the probes need be processed so that all the indices and parameters of interest can be extrapolated from it. A low-pass Hamming filter with a cut-off frequency of 400Hz is applied to the 'raw' signal, suppressing all frequency components of the signal above the cut-off frequency and preserving only the lower frequency components. The filter thus eliminates high frequency noise and prevents aliasing[5]. The Sampling Theorem (or Nyquist- Shannon's) states that the

[5] Aliasing: the phenomenon whereby two different analogue signals are indistinguishable once they have been sampled. This is due to undersampling of the signal. The term is coined from the fact that

minimum frequency required to sample a signal without loss of information is at least twice the maximum frequency of the signal. It is therefore fundamental to eliminate all noise at a frequency higher than the frequency of the signal of interest, which for most muscles is around 400Hz (Merletti R, et al., 2004). The signal is then filtered a second time, again using a high-pass Hamming filter with a cut-off frequency of 20Hz. This pass is used to eliminate signal harmonics resulting from both motion artefacts and noise induced by the intrinsic instability present at the electrode-skin interface (Merletti R, et al., 2004, Ranavolo A et al., 2021). At the output of the wave-pass filter resulting from the union of the two previous filters, the signal undergoes a rectification[6] operation, then a final 5Hz low-pass Hamming filter is applied to obtain the envelope.

Another significant step in sEMG signal processing is amplitude normalisation. Amplitude normalisation consists of dividing the previously processed sEMG signal by a reference value so that the resulting signal is expressed as a percentage of the reference value used, providing information about the magnitude of muscle activation referred to a reference value (Besomi M et al., 2020). The literature shows that there are various normalisation methods that differ depending on the reference value chosen. Another important consideration is that there is no consensus in the scientific world as to which is the most appropriate and optimal normalisation method to use (Ranavolo A et al., 2021). In this study, $Peak_{task}$ (peak task) was used, which involves normalisation according to the maximum peak value of each trial of a patient task. The purpose of sEMG amplitude normalisation is to allow comparison of:

- signals recorded by several participants;
- signals from different muscles;
- individual measurements or with repositioning of the electrodes.

Thus, normalising in amplitude allows minimising non-congruities (discrepancies) due to various aspects, such as: anatomical and physiological characteristics of the muscles and technical aspects (Besomi M et al., 2020, Ranavolo A et al., 2021).

The final step in the data analysis was the calculation of the muscle coactivation curves and the corresponding indices. Of the several methodologies for calculating

higher frequency components 'hide' behind the lower frequencies where they overlap, assuming a false identity (aliasing).

[6] Rectification is the application of a modulus function to the signal, thus making all samples positive.

coactivation, we chose to use those that did not require an a priori assumption about the type of function or activity performed by the muscles or muscle groups (e.g. muscle 1 antagonist and muscle 2 agonist). The methods we used were therefore the time-varying Rudolph approach (Rudolph K S et al., 2000) and the time-varying multi-muscle co-activation function "TMCf(d(t),t)" (Ranavolo A et al., 2015).

- Rudolph: This approach provides a continuous sample-by-sample evaluation of the relative activation of the pair of muscles and the extent of cocontraction during the observation period of the task, which enables the construction of a cocontraction curve. The formula is as follows:

$$C(i) = \frac{\min\left[EMG(i)_{G1}, EMG(i)_{G2}\right]}{\max\left[EMG(i)_{G1}, EMG(i)_{G2}\right]} \cdot \left(\frac{EMG(i)_{G1} + EMG(i)_{G2}}{2}\right)$$

$EMG(i)_{G1}, EMG(i)_{G2}$ indicate the two muscles. If you want to calculate the co-activation of more than two muscles, you need to construct two muscle groups, as this algorithm only provides two inputs. The numerator of the fraction indicates the activity of the less active muscle, while the denominator represents the activity of the more active muscle, thus avoiding division by zero errors. The ratio is multiplied by half the sum of the activities found in the two muscles. The summed activity of the two muscles is divided by 2 to obtain coactivation values ranging from 0 to 100. The one presented is a variation of the formula for coercion proposed by Rudolph and colleagues, precisely the halving of the sum of muscle activities (Rudolph K S et al., 2000, Ranavolo A et al., 2021).

When the formula yields high coactivation values, it means that a high level of activation of both muscles occurred during the task. If the cocontraction values are low, then either there was a low activation of both muscles, or one muscle presented a high activation, while the other showed a low activation (Rudolph K S et al., 2000).

From the coactivation curve, thus calculated, it is possible to extrapolate an index that summarises the cocontraction of the muscles under examination.

$$CI = \frac{\sum_{i=1}^{N} C(i)}{N}$$

The Co-Activation Index (CI) is calculated by averaging the function over the duration of the task (Ranavolo A et al., 2021). Since, as mentioned above, the function proposed by Rudolph and colleagues only provides two input data, the mean values of the right and left erector spinae longissimus (the extensor) and right and left rectus abdominis superior (the flexor) activations were included in this study. The mean activations were calculated after previous normalisation in time and amplitude.

- Time-varying multi-muscle co-activation function: The second method used (TMCf(d(t),t)) has the same features as the algorithm proposed by Rudolph and colleagues, except that it enables the evaluation of coactivations on more than two muscles (muscle groups) simultaneously. In this case, the function is expressed as follows:

$$TMCf(d(i), i) = C\big(d(i)\big) \cdot m(i) \cdot cc(i)$$

Where $C\big(d(i)\big)$ is a sigmoidal curve[7] and assumes values in the range 0,1.

$$C\big(d(i)\big) = \left(1 - \frac{1}{1 + e^{-12(d(i)-0.5)}}\right)$$

The $C\big(d(i)\big)$ function incorporates, in the exponential function argument, the average of the differences of each pair of EMG samples ($d(i)$).

$$d(i) = \left(\frac{\sum_{m=1}^{M-1} \sum_{j=m+1}^{M} \left| EMG_m(i) - EMG_j(i) \right|}{100 \cdot \frac{M!}{2! \cdot (M - 2!)}} \right)$$

[7] A sigmoidal curve, also known as the 'standard logistic function', is a function that is: (1) continuous; (2) derivable; (3) continuously differentiable; (4) has a single inflection point; (5) has a non-negative first derivative (Hui Liu, 2020).

Where M represents the number of muscles examined, while $\frac{M!}{2!\cdot(M-2!)}$ calculates the total number of differences between each pair of $EMG_i(t)$.

Due to the sigmoid weight coefficient ($C(d(i))$), the TMCf algorithm has the following characteristics:

a. inversely proportional relationship with the mean of the differences $d(i)$ between each pair of $EMG_m(i)$;
b. assumes values close to the value assumed by the muscles $m(i)$ when the mean of the differences $d(i)$ is close to zero and values close to zero when $d(i)$ is close to 1.

Therefore, the smaller the differences between the various muscle activations, the more $d(i)$ will take on values close to zero and consequently $C(d(i))$ will tend to 1, resulting in TMCf values approximating (close) to the product $m(i) \cdot cc(i)$. As the differences between the muscle activations increase, $C(d(i))$ will decrease causing a consequent reduction in the TMCf values.

$$m(i) = \frac{\sum_{m=1}^{M} EMG_m(i)}{M}$$

where: $EMG_m(i)$ indicates the amplitude of the m-th signal at the i-th instant, while M is the number of muscles considered. $m(i)$ essentially estimates the average behaviour of the M muscles.

Finally, the term $cc(i)$ is a correction coefficient for the adjustment of the TMCf formula in the case where the input muscles are only two in number:

$$cc(i) = \frac{\left(\frac{\sum_{m=1}^{M} EMG_m(i)}{M}\right)}{max_{m=1\ldots M}[EMG_m(i)]}$$

(Ranavolo A et al., 2015, Ranavolo A et al., 2021).

The parameters of interest that were extrapolated from the acquired data are: average, maximum and full width at half maximum (FWHM). The three parameters were calculated for: muscle activations; muscle co-activations calculated using the method of Rudolph and colleagues; muscle co-activations calculated using the TMCf algorithm. The FWHM is the range in which the activation curve (or co-activation curve) lies above half of its maximum value (Varrecchia T et al, 2018).

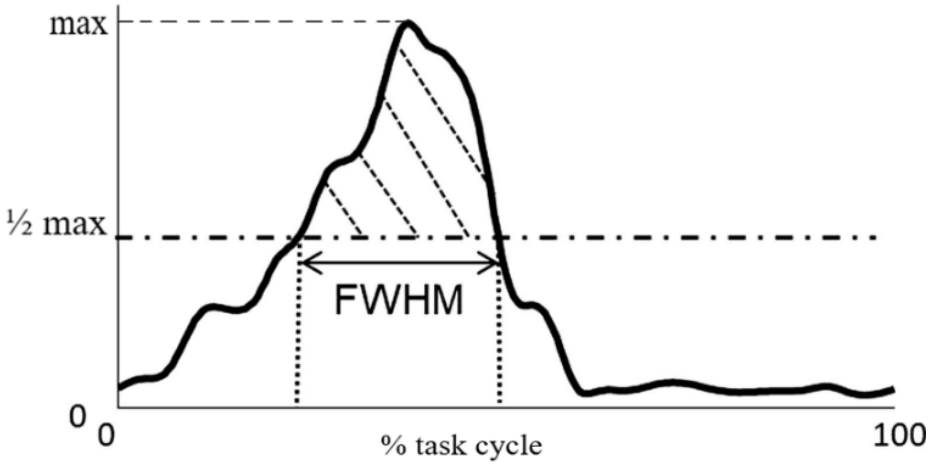

Figure 4 Example of Full Width at Half Maximum (FWHM) plotted.

Statistical Analysis

To make a statistical inference means to deduce the characteristics of a population from a sample of that same population. Indeed, the word infer comes from the Latin *inferre*, which means "to bring in", inferential statistics brings in the characteristic of a sample into the population. Statistical tests are based on inverse logic, so for our thesis to be verified, we want the test to reject the null hypothesis. In particular, the pivotal parameters of any hypothesis test are:

- H_0: the null hypothesis, the one that the test is designed to prove.
- H_a: the alternative hypothesis that is proposed by the person performing the test for the population and that is tested by the test itself. Is the hypothesis on which the inference is made.
- p-value: the probability that, under the assumption that H_0 is true, each value obtained from the test statistic is greater than or equal to the observed value.
- α: the significance level, the threshold value against which the p-value is compared.

The comparison between p-value and alpha reveals the result of the hypothesis test. If $p < \alpha$ the test rejects H_0; if else $p > \alpha$ the test does not reject H_0. To analyse the results of this study, the α significance level was set at 0.05 (5%) for each tests.

The statistical evaluation of the sample analysed was carried out by first applying the Shapiro-Wilk test to check whether the data followed a normal distribution. Indeed, the null hypothesis of the Shapiro-Wilk test is: "The vector composed of the samples is normal with unspecified mean and variance". Especially for the analysis of small samples, the Shapiro-Wilk test proves to be very powerful.

Depending on the results obtained with the Shapiro-Wilk test, either the 2-sample paired t-test or the Wilcoxon signed rank test is used to analyse all of the calculated parameters. The t-test is a statistical hypothesis test used to compare the means of two groups. T-tests are parametric, which means that they can be used when the samples meet the conditions of normality, equal variance and independence (Kim TK, 2015). Since we need to compare the magnitude of variation between the pre- and post-vertebroplasty states for the same subjects, a paired t-test is used. The Wilcoxon signed rank test is a non-parametric test often used for paired data, such as comparing pre- and post-treatment measurements (Rosner B et al., 2006). Usually, non-parametric methods, such as the one proposed by Wilcoxon, are based on the sorting of the data according to their size and the substitution of the observed values by the number of ranks (Dexter F, 2013).

The two methods of calculating co-activations (Rudolph and TMCf) were also compared statistically. Both Wilcoxon signed ranked and Mann-Whitney tests were used for this purpose. The Mann-Whitney U test, commonly known as the Wilcoxon rank-sum test, is the analogue of the parametric Student's t-test for non-parametric

distributions. In actual fact, it compares the means of two independent groups, assuming that the data do not have a Gaussian distribution (Dehaene H et al., 2021, Sundjaja JH et al., 2022).

The tests described above have been implemented in MATLAB using the following functions of the Statistics and Machine Learning Toolbox:

- *[H, pValue, W] = swtest(X, alpha)* (Shapiro-Wilk), which takes as input a vector with the samples to be analysed (the function requires X to be a column vector with at least 3 elements and at most 5000), while alpha is a scalar set to 0.05. The outputs of this function are H, which can only take the values 0 or 1 (if H = 0 the test does not reject the null hypothesis at significance level α, while if H = 1 the test rejects the null hypothesis at significance level α), the p-value and the statistic W, which can be interpreted as the square of the correlation coefficient in a quantile-quantile plot, W can take values between 0 and 1 (if the value of W is close to 0, the test rejects the null hypothesis).

- *[p,h] = signrank(X, Y)* (Wilcoxon), which provides two input vectors of equal size, in this study X contains the means of the summary index of the sample to be analysed in the pre-vertebroplasty condition, while Y contains the same means in the post-vertebroplasty condition. The null hypothesis is: "The difference of the input vectors (X-Y) comes from a distribution with zero median". The function yields as output the p-value of a pairwise, two-sided test and a logical value indicating the test decision (h = 1 indicates rejection of the null hypothesis, while h = 0 indicates no rejection of the null hypothesis at the default 5% significance level).

- *[p,h] = ranksum(X, Y)*(Mann-Whitney) is a two-sided Wilcoxon rank sum test and tests the null hypothesis that the input vectors contain samples from continuous distributions with equal medians. Since the test assumes that the samples are independent, the input vectors X and Y can have different lengths. The outputs of the function are the p-value and the logical value h indicating the decision of the test (if h=1, the test rejects the null hypothesis, if h=0, the null hypothesis cannot be rejected). The significance level is set to 5%

3. Results

In this section, the results obtained are presented in the form of a histogram with corresponding error bars for each task. For every task, the results of each parameter are reported for both activations and co-activations, comparing pre- and post-treatment conditions. For the lifting task, it was decided to report the results not only by comparing the pre- and post-vertebroplasty condition, but also by adding the comparison with the healthy condition presented by the control subjects. The tables (Tab.1-Tab.4) show the p-values returned by the Wilcoxon signed rank test for each task and for each index of muscle activation and co-activation.

- LIFTING

p-value	ES	RAS	TMCf	Rudolph
MEAN	0.56	0.22	0.75	0.75
MAX	0.44	0.69	0.75	0.5
FWHM	0.19	0.16	0.5	0.75

Table 1.

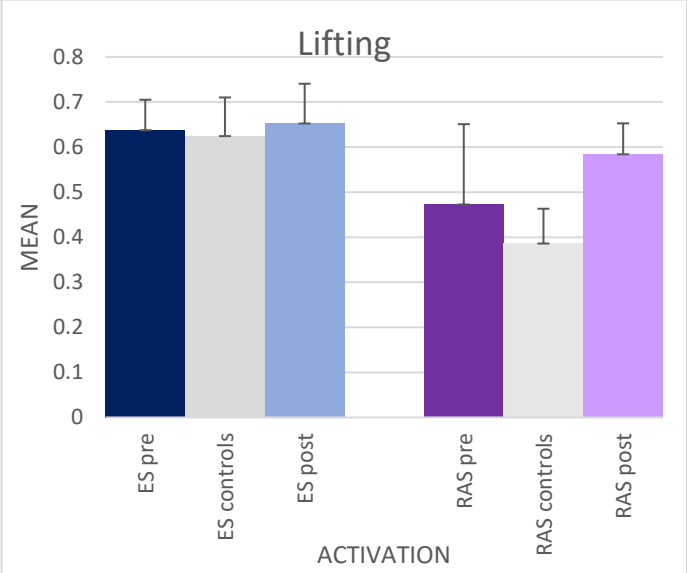

Figure 5 Histogram of average ES and RAS activations of patients before and after vertebroplasty and healthy subjects in the lifting task.

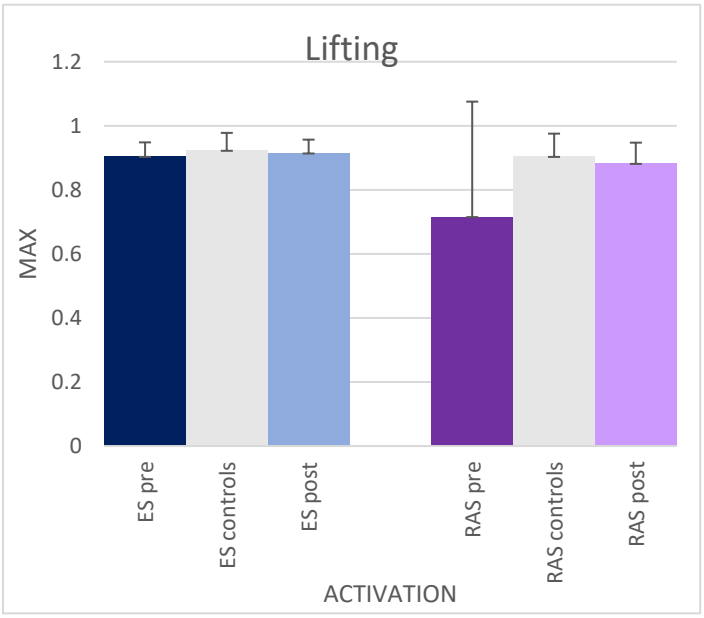

Figure 5 Histogram of maximum ES and RAS activations in patients before and after vertebroplasty and in healthy subjects during the lifting task.

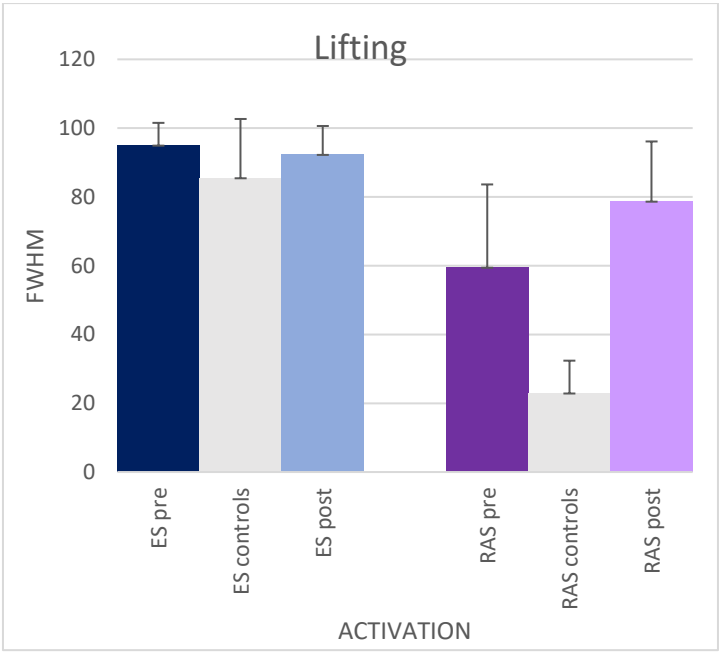

Figure 7 FWHM histogram of ES and RAS activations in pre- and post-vertebroplasty patients and healthy subjects during the lifting task.

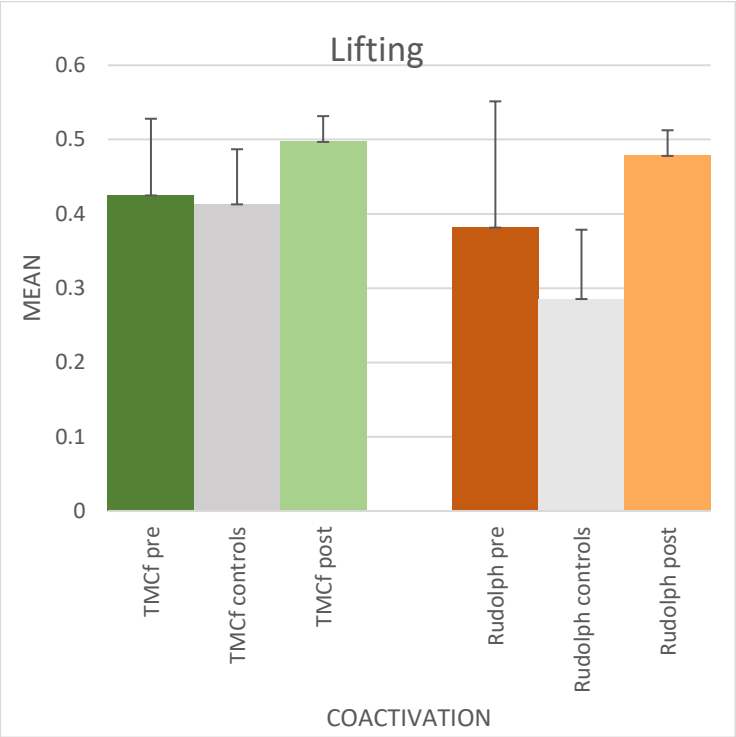

Figure 6 Histogram of mean coactivations with TMCf and Rudolph in patients before and after vertebroplasty and healthy subjects in the lifting task.

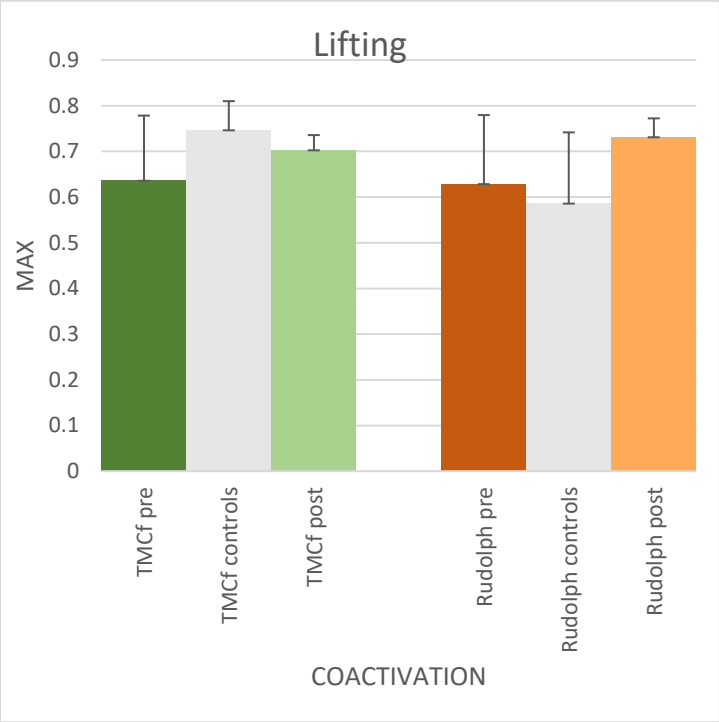

Figure 7 Histogram of maximum coactivations with TMCf and Rudolph in patients before and after vertebroplasty and healthy subjects in the lifting task.

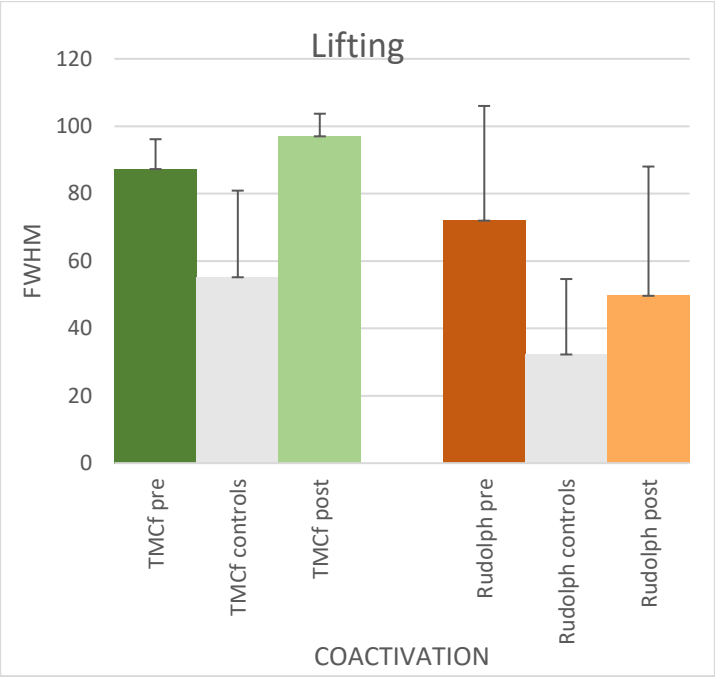

Figure 10 FWHM histogram of TMCf and Rudolph co-activations of patients before and after vertebroplasty and healthy subjects in the lifting task.

- LOWERING

p-value	ES	RAS	TMCf	Rudolph
MEAN	0.56	0.56	0.5	1
MAX	0.84	0.69	0.75	0.75
FWHM	0.69	0.44	0.5	0.25

Table 2.

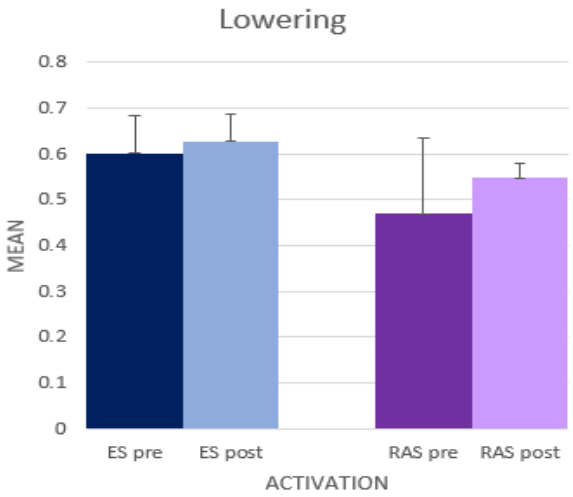

Figure11 Histogram of average ES and RAS activations of patients before and after vertebroplasty in the lowering task.

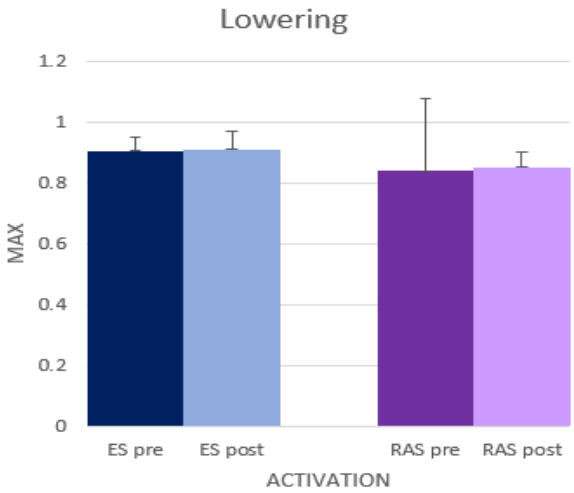

Figure12 Histogram of maximum ES and RAS activations of patients before and after vertebroplasty in the lowering task.

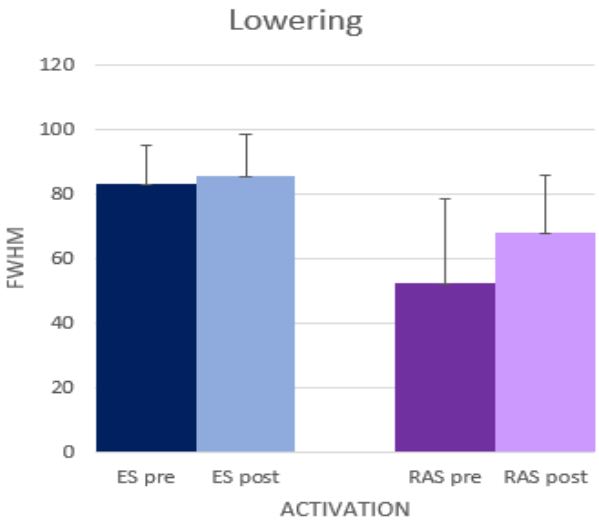

Figure 13 FWHM histogram of ES and RAS activations in pre- and post-vertebroplasty patients during the lowering task.

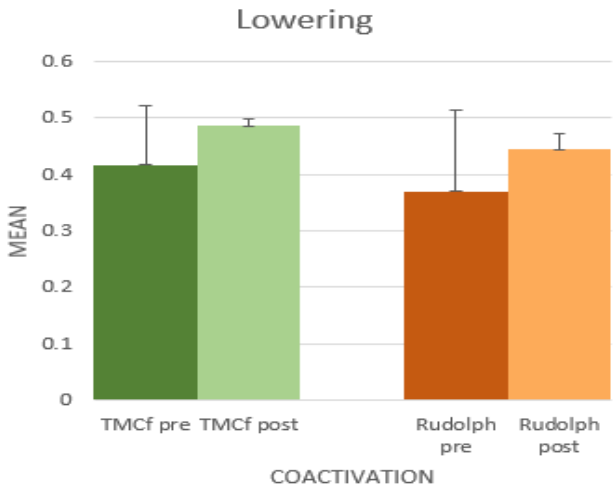

Figure 14 Histogram of mean coactivations with TMCf and Rudolph in patients before and after vertebroplasty in the lowering task.

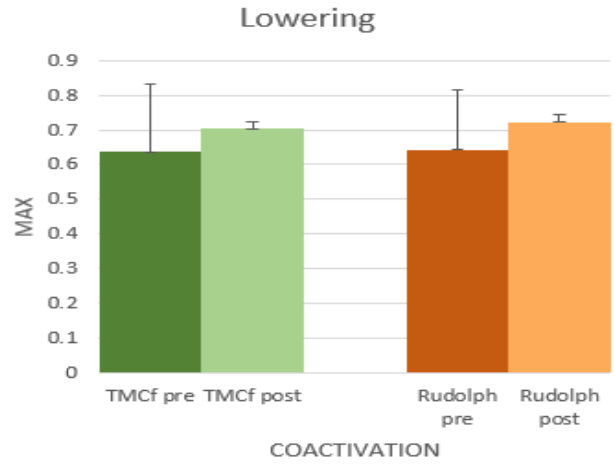

Figure 15 Histogram of maximum coactivations with TMCf and Rudolph in patients before and after vertebroplasty in the lowering task.

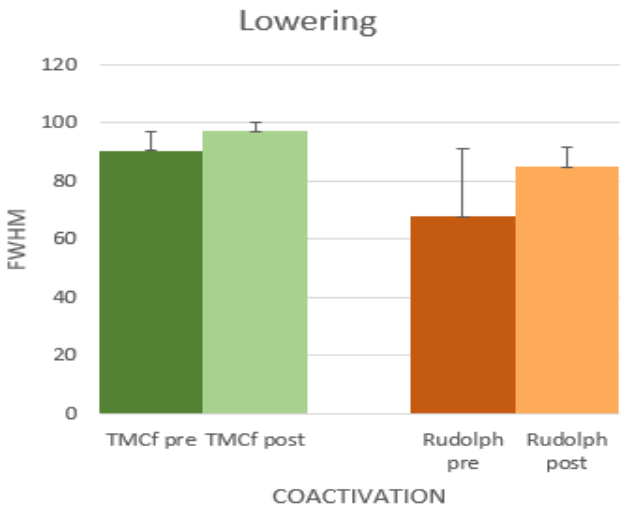

Figure 16 FWHM histogram of TMCf and Rudolph co-activations of patients before and after vertebroplasty in the lowering task.

- SIT TO STAND

p-value	ES	RAS	TMCf	Rudolph
MEAN	0.64	0.95	1	1
MAX	0.19	0.19	0.63	0.63
FWHM	0.55	0.19	0.88	0.5

Table 3.

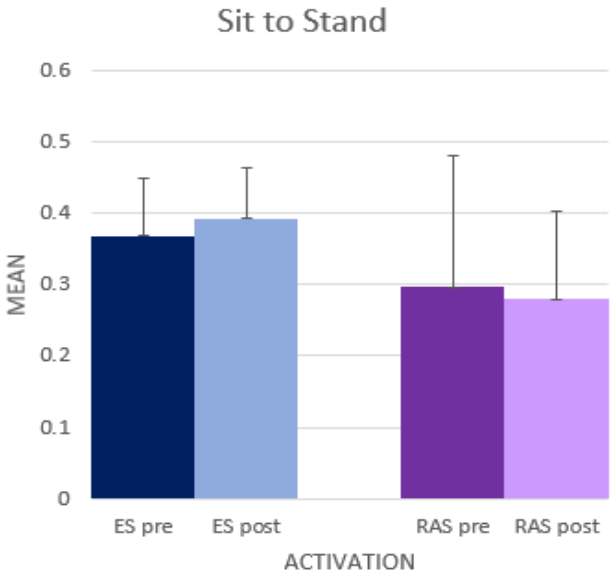

Figure 17 Histogram of average ES and RAS activations of patients before and after vertebroplasty in the Sit to Stand task.

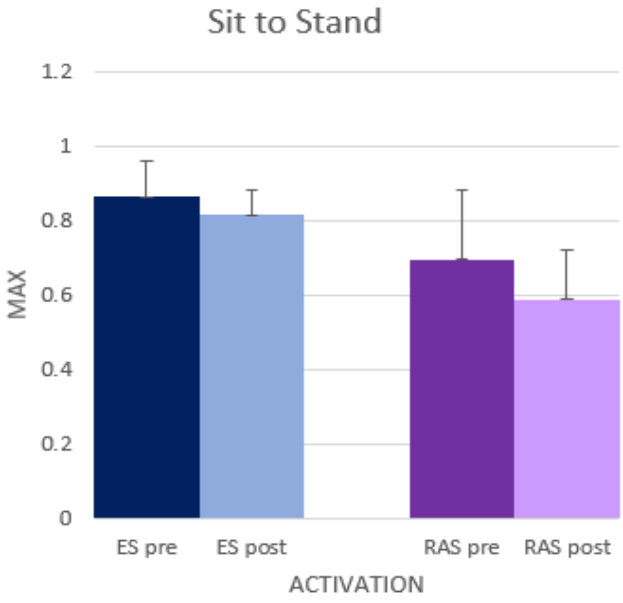

Figure 18 Histogram of maximum ES and RAS activations of patients before and after vertebroplasty in the Sit to Stand task.

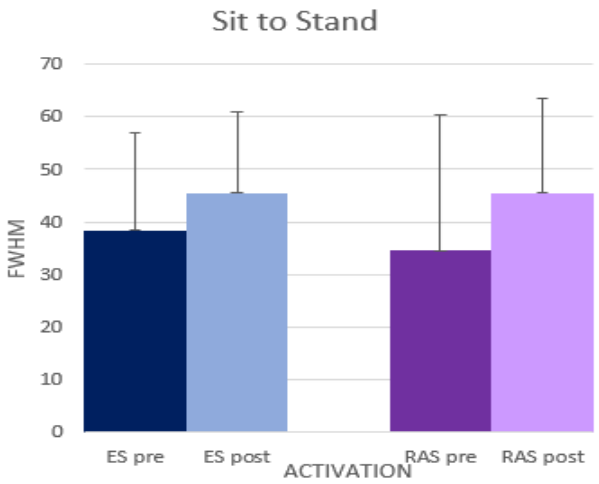

Figure 19 FWHM histogram of ES and RAS activations in pre- and post-vertebroplasty patients during the Sit to Stand task.

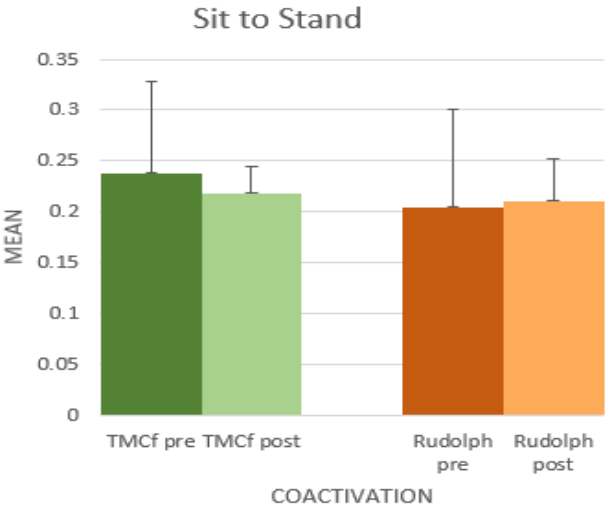

Figure 20 Histogram of mean coactivations with TMCf and Rudolph in patients before and after vertebroplasty in the Sit to Sta task.

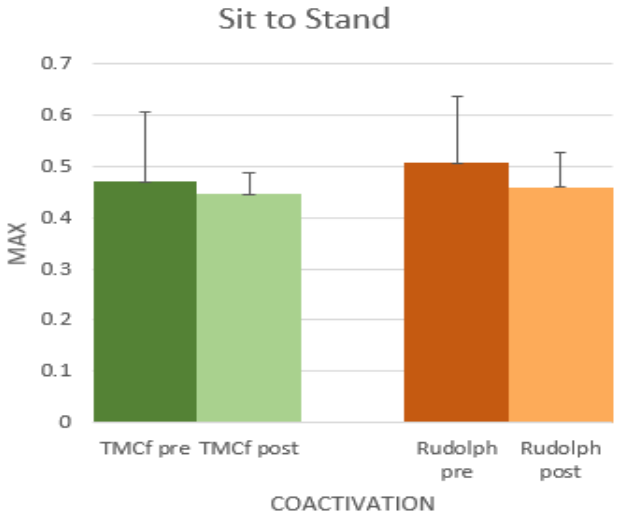

Figure 21 Histogram of maximum coactivations with TMCf and Rudolph in patients before and after vertebroplasty in the Sit to Sta task.

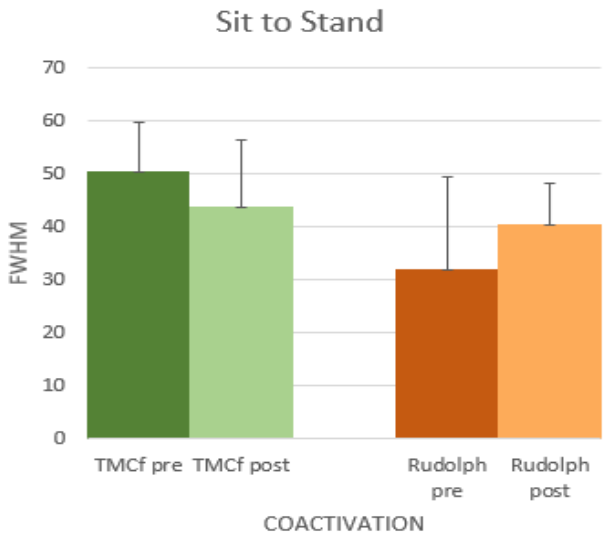

Figure 22 FWHM histogram of TMCf and Rudolph co-activations of patients before and after vertebroplasty in the Sit to Stand task.

- STAND TO SIT

p-value	ES	RAS	TMCf	Rudolph
MEAN	0.31	0.44	0.75	1
MAX	1	0.16	0.5	0.5
FWHM	0.84	0.56	0.75	0.5

Table 4.

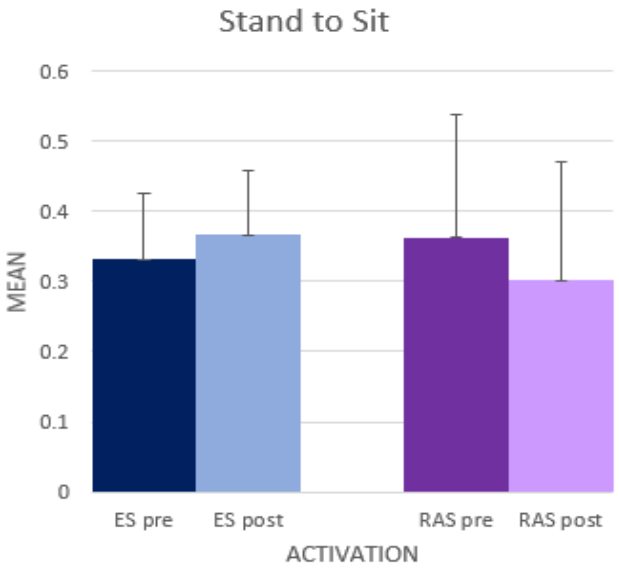

Figure 23 Histogram of mean ES and RAS activations of patients before and after vertebroplasty in the Stand to Sit task.

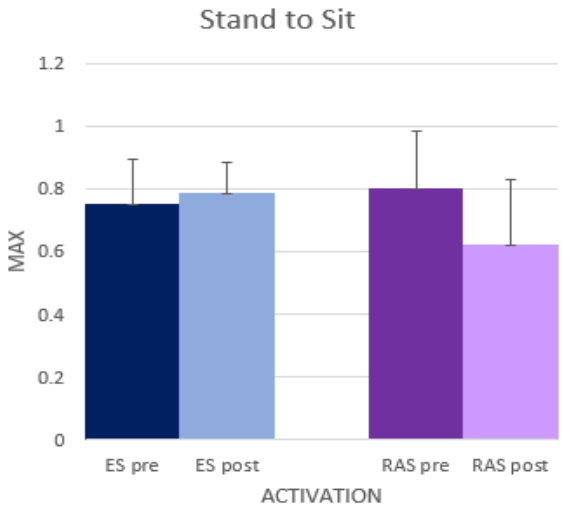

Figure 24 Histogram of maximum ES and RAS activations of patients before and after vertebroplasty in the Stand to Sit task.

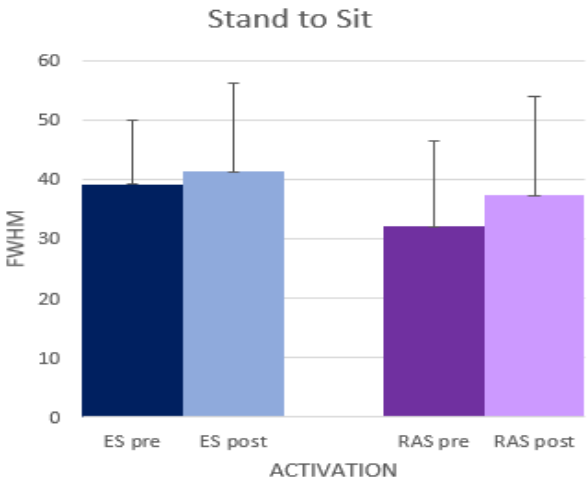

Figure 25 FWHM histogram of ES and RAS activations in pre- and post-vertebroplasty patients during the Stand to Sit task.

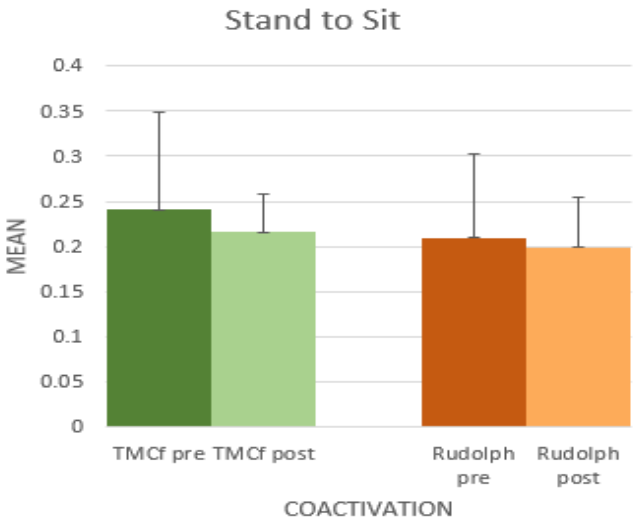

Figure 26 Histogram of mean coactivations with TMCf and Rudolph in patients before and after vertebroplasty in the Stand to Sit task.

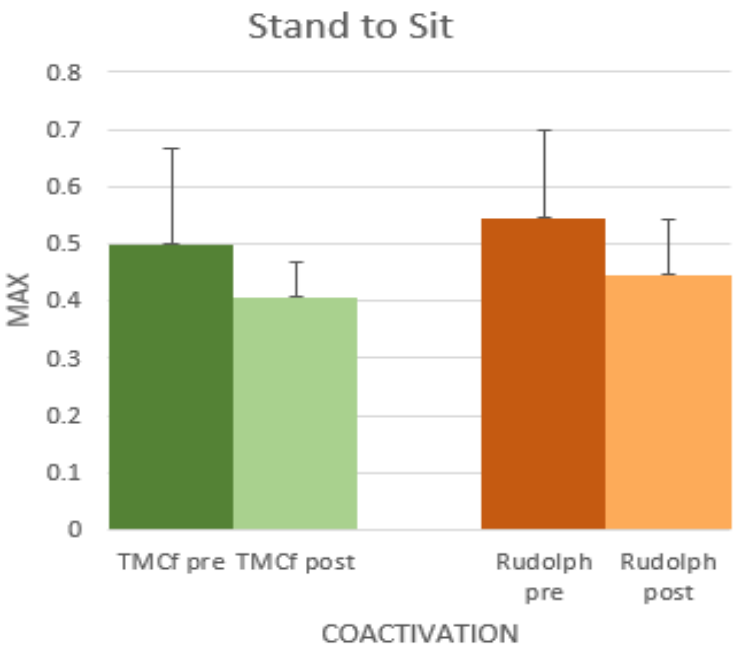

Figure 27 Histogram of maximum coactivations with TMCf and Rudolph in patient before and after vertebroplasty in the Stand to Sit task.

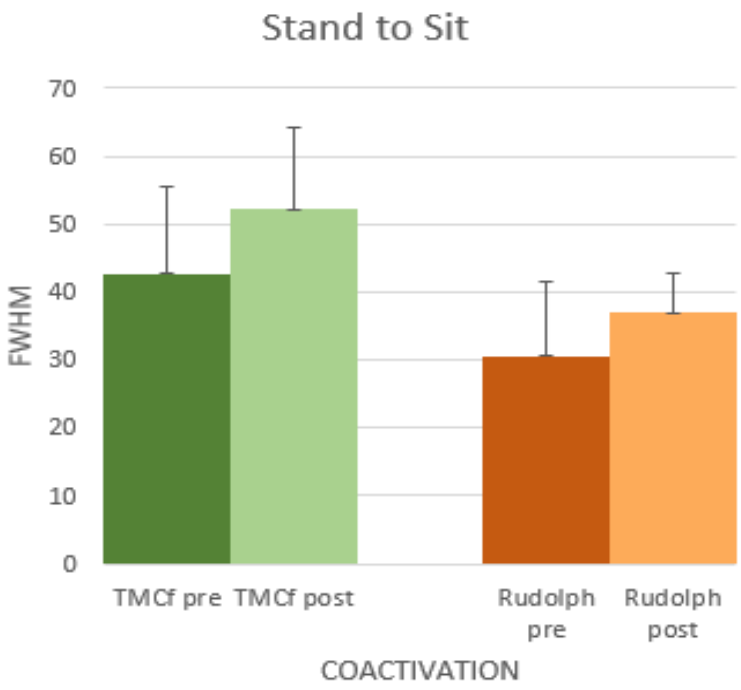

Figure 28 FWHM histogram of TMCf and Rudolph co-activations of patients before and after vertebroplasty in the *Stand to Sit task*.

The p-value results for the evaluation of the two algorithms for the calculation of coactivations returned by the statistical analysis are shown below:

PRE	Wilcoxon test	Mann-Whitney test	POST	Wilcoxon test	Mann-Whitney test
Lifting MEAN	0.5	1		0.5	0.7
Lifting MAX	0.5	1		0.25	0.4
Lifting FWHM	0.75	1		0.25	0.2
Lowering MEAN	0.25	0.7		0.25	0.1
Lowering MAX	0.75	1		0.75	0.4
Lowering FWHM	0.25	0.1		0.25	0.1
Sit to Stand MEAN	0.25	0.69		0.88	1
Sit to Stand MAX	0.13	0.69		0.38	0.49
Sit to Stand FWHM	0.13	0.2		0.88	0.69
Stand to Sit MEAN	0.25	0.7		0.5	1
Stand to Sit MAX	0.25	0.7		0.25	0.7
Stand to Sit FWHM	0.25	0.7		0.25	0.1

Table 5.

4. Discussion

The Shapiro-Wilk test did not allow us to conclude that all the samples analysed followed a normal trend, consequently, the parameters were analysed using the non-parametric Wilcoxon and Mann-Whitney tests.

The results reveal an overall increase in the activations of the two muscle groups observed and, consequently, an increase in their co-activations after the vertebral consolidation procedure. There are two possible explanations for this increase:

- In the pre-vertebroplasty state, the central nervous system is inhibited by the disease, so that the activations and coactivations, although lower, indicate that the central nervous system is behaving pathologically.
- At the time of post-vertebroplasty acquisition, 30 days after surgery, the increase in activations and coactivations indicates that the patient needs immediate personalised rehabilitation treatment.

In order to understand which of the above hypotheses is the acceptable one, the results for the lifting task were compared with those calculated for healthy controls. If the post-operative condition most closely resembles the behaviour of the controls, this results in an initial inhibition of the CNS, so that vertebroplasty increases the activation and coactivation values and brings them back to normal levels. Conversely, after the operation, the CNS activates the trunk muscles to a greater extent in order to protect the spine, but this can lead to many disadvantages, which we have already discussed in the introductory section. The post-vertebroplasty period is therefore a very delicate phase in which this increased co-activation requires to be counteracted from the outset by means of appropriate rehabilitation treatment.

Comparison with healthy subjects showed that the patients' muscular behaviour was more akin to that of the controls, before the spinal consolidation procedure. Therefore, it is of paramount importance to provide patients with appropriate treatment at an early stage after surgery.

Especially for the lifting and lowering task, the increase in mean activations (Fig. 5; Fig. 11) and mean coactivations (Fig. 8; Fig. 14) after the intervention is noticeable. On the other hand, for the sit-to-stand and stand-to-sit tasks, it is observed that the

CNS increases the recruitment of the paravertebral muscles (right and left erector spinae longissimus) in the aftermath of vertebroplasty (Fig. 17; Fig. 23). Increased co-activation and activity of the ES and RAS antagonist muscles results in increased trunk stiffness (Lee PJ et al., 2006, Latash ML, 2018). Trunk stiffness is a major contributor to spinal stability. Stability describes the ability to maintain balance in the presence of kinematic and/or control impairments. The contribution of muscle co-contraction to trunk stiffness is due to the fact that stiffness is mainly associated with the active muscles of the trunk musculature rather than the passive tissues (Lee PJ et al., 2006).

Furthermore, the scientific scenario indicates that co-activation contributes to a reduction in net moments at the L5-S1 joint and a 12-18% increase in spinal load, which in turn leads to an increased risk of low-back disorders (LBDs) (Ranavolo A et al., 2018). It follows that in the post-vertebroplasty condition, the lumbar spine is subject to significant compressive and shearing forces, which implies a greater risk of injury and increased pain (Varecchia T et al., 2022).

Regarding the comparison between the function proposed by Rudolph and colleagues and the TMCf for calculating coactivation curves, the absence of statistical significance (shown in Table 5) indicates that, as this study was designed, the two methods are equivalent. If a study were set up differently, e.g. with a wider number of muscles, this conclusion would not be valid.

5. Limitations

A significant limitation of this study is the small number of patients who were enrolled in the study sample up to this point to the experimental phase. It is precisely because of this narrow sample size that no statistical significance was revealed.

An important artefact in the data of this study is the contamination of the electrocardiogram (ECG) affecting the two superior rectus abdominis muscles. This contamination is a consequence of the proximity of the surface electrodes to the heart and the volume conduction properties of human tissue. For the tasks performed in this study, which require modest muscle activation, the amplitudes of the sEMG signals are considerably affected by the ECG artefact (Butler HL et al., 2009). Complete removal of the ECG contribution to the signal is particularly complex due to the overlapping frequency spectrum of sEMG (20-500 Hz) and ECG (0-200 Hz) signals (Butler HL et al., 2009, Christov II et al., 1999). Since the majority of sEMG power is found between 20 and 200 Hz, while the majority of ECG power falls below 35 Hz, the presence of the ECG can result in an increase in the power of frequencies in the lower region of the sEMG spectrum and distort the amplitude of the sEMG, contaminating the information of interest from the abdominal muscles (Drake JD et al., 2006). The literature shows that in non-fatiguing regimes, such as those proposed in this study, the use of a high cut-off reduces ECG contamination, but also leads to a reduction in amplitude and attenuation of the signal of interest, with consequent loss of information (Redfern M et al., 1993, Drake JD et al., 2006). As mentioned in paragraph 2.4, the high-pass Hamming filter used has a cut-off frequency of 20 Hz.

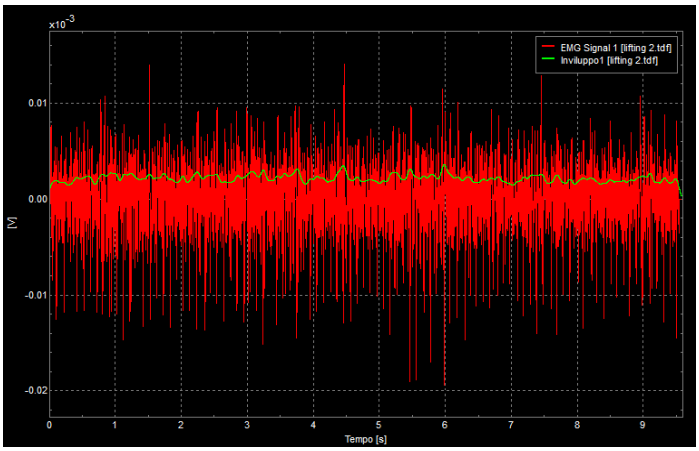

Figure 8. The image represents the raw sEMG signal acquired by the RAS in red, and the envelope of the same processed signal in green.

BIOGRAPHY:

1. Anderson KC, Auclair D, Adam SJ, Agarwal A, Anderson M, Avet-Loiseau H, Bustoros M, Chapman J, Connors DE, Dash A, Di Bacco A, Du L, Facon T, Flores-Montero J, Gay F, Ghobrial IM, Gormley NJ, Gupta I, Higley H, Hillengass J, Kanapuru B, Kazandjian D, Kelloff GJ, Kirsch IR, Kremer B, Landgren O, Lightbody E, Lomas OC, Lonial S, Mateos MV, Montes de Oca R, Mukundan L, Munshi NC, O'Donnell EK, Orfao A, Paiva B, Patel R, Pugh TJ, Ramasamy K, Ray J, Roshal M, Ross JA, Sigman CC, Thoren KL, Trudel S, Ulaner G, Valente N, Weiss BM, Zamagni E, Kumar SK. Minimal Residual Disease in Myeloma: Application for Clinical Care and New Drug Registration. Clin Cancer Res. 2021 Oct 1;27(19):5195-5212. doi: 10.1158/1078-0432.CCR-21-1059. PMID: 34321279; PMCID: PMC9662886.

2. Argyriou AA, Iconomou G, Kalofonos HP. Bortezomib-induced peripheral neuropathy in multiple myeloma: a comprehensive review of the literature. Blood. 2008 Sep 1;112(5):1593-9. doi: 10.1182/blood-2008-04-149385. Epub 2008 Jun 23. Erratum in: Blood. 2009 Apr 30;113(18):4478. PMID: 18574024.

3. Besomi M, Hodges PW, Clancy EA, Van Dieën J, Hug F, Lowery M, Merletti R, Søgaard K, Wrigley T, Besier T, Carson RG, Disselhorst-Klug C, Enoka RM, Falla D, Farina D, Gandevia S, Holobar A, Kiernan MC, McGill K, Perreault E, Rothwell JC, Tucker K. Consensus for experimental design in electromyography (CEDE) project: Amplitude normalization matrix. J Electromyogr Kinesiol. 2020 Aug;53:102438. doi: 10.1016/j.jelekin.2020.102438. Epub 2020 Jun 10. PMID: 32569878.

4. Butler HL, Newell R, Hubley-Kozey CL, Kozey JW. The interpretation of abdominal wall muscle recruitment strategies change when the electrocardiogram (ECG) is removed from the electromyogram (EMG). J Electromyogr Kinesiol. 2009 Apr;19(2):e102-13. doi: 10.1016/j.jelekin.2007.10.004. Epub 2007 Dec 4. PMID: 18055221.

5. Castillo JJ. Plasma Cell Disorders. Prim Care. 2016 Dec;43(4):677-691. doi: 10.1016/j.pop.2016.07.002. Epub 2016 Oct 14. PMID: 27866585.

6. Chen B, Cai L, Zhou F. Management of acute spinal cord compression in multiple myeloma. Crit Rev Oncol Hematol. 2021 Apr;160:103205. doi: 10.1016/j.critrevonc.2020.103205. Epub 2020 Dec 30. PMID: 33387626.

7. Chen LH, Hsieh MK, Niu CC, Fu TS, Lai PL, Chen WJ. Percutaneous vertebroplasty for pathological vertebral compression fractures secondary to multiple myeloma. Arch Orthop Trauma Surg. 2012 Jun;132(6):759-64. doi: 10.1007/s00402-012-1474-y. Epub 2012 Feb 8. PMID: 22314399.

8. Christov II, Daskalov IK. Filtering of electromyogram artifacts from the electrocardiogram. Med Eng Phys. 1999 Dec;21(10):731-6. doi: 10.1016/s1350-4533(99)00098-3. PMID: 10717553.

9. Croucher PI, Apperley JF. Bone disease in multiple myeloma. Br J Haematol. 1998 Dec;103(4):902-10. doi: 10.1046/j.1365-2141.1998.01082.x. PMID: 9886299.

10. Dehaene H, De Neve J, Rosseel Y. A Wilcoxon-Mann-Whitney Test for Latent Variables. Front Psychol. 2021 Nov 15;12:754898. doi: 10.3389/fpsyg.2021.754898. PMID: 34867650; PMCID: PMC8634887.

11. Dexter F. Wilcoxon-Mann-Whitney test used for data that are not normally distributed. Anesth Analg. 2013 Sep;117(3):537-538. doi: 10.1213/ANE.0b013e31829ed28f. PMID: 23966647.

12. Drake JD, Callaghan JP. Elimination of electrocardiogram contamination from electromyogram signals: An evaluation of currently used removal techniques. J Electromyogr Kinesiol. 2006 Apr;16(2):175-87. doi: 10.1016/j.jelekin.2005.07.003. Epub 2005 Aug 31. PMID: 16139521.

13. Hermens HJ, Freriks B, Disselhorst-Klug C, Rau G. Development of recommendations for SEMG sensors and sensor placement procedures. J Electromyogr Kinesiol. 2000 Oct;10(5):361-74. doi: 10.1016/s1050-6411(00)00027-4. PMID: 11018445.

14. Hui Liu, Chapter 7 - Rail transit channel robot systems, Editor(s): Hui Liu, Robot Systems for Rail Transit Applications, Elsevier, 2020, Pages 283-328

15. Kim TK. T test as a parametric statistic. Korean J Anesthesiol. 2015 Dec;68(6):540-6. doi: 10.4097/kjae.2015.68.6.540. Epub 2015 Nov 25. PMID: 26634076; PMCID: PMC4667138.

16. Kristinsson SY, Landgren O, Dickman PW, Derolf AR, Björkholm M. Patterns of survival in multiple myeloma: a population-based study of patients diagnosed in Sweden from 1973 to 2003. J Clin Oncol. 2007 May 20;25(15):1993-9. doi: 10.1200/JCO.2006.09.0100. Epub 2007 Apr 9. PMID: 17420512.

17. Larsen RF, Jarden M, Minet LR, Frølund UC, Möller S, Abildgaard N. Physical function in patients newly diagnosed with multiple myeloma; a Danish cohort study. BMC Cancer. 2020 Mar 3;20(1):169. doi: 10.1186/s12885-020-6637-6. PMID: 32126972; PMCID: PMC7055017.

18. Latash ML. Muscle coactivation: definitions, mechanisms, and functions. J Neurophysiol. 2018 Jul 1;120(1):88-104. doi: 10.1152/jn.00084.2018. Epub 2018 Mar 28. PMID: 29589812; PMCID: PMC6093955.

19. Lee PJ, Rogers EL, Granata KP. Active trunk stiffness increases with co-contraction. J Electromyogr Kinesiol. 2006 Feb;16(1):51-7. doi: 10.1016/j.jelekin.2005.06.006. Epub 2005 Aug 15. PMID: 16099678; PMCID: PMC1635026.

20. Marjanović S, Mijusković Z, Stamatović D, Madjaru L, Ralić T, Trimcev J, Stojanović J, Radović V 2nd. Multiple myeloma invasion of the central nervous system. Vojnosanit Pregl. 2012 Feb;69(2):209-13. PMID: 22500379.

21. McDonald RJ, Trout AT, Gray LA, Dispenzieri A, Thielen KR, Kallmes DF. Vertebroplasty in multiple myeloma: outcomes in a large patient series. AJNR Am J Neuroradiol. 2008 Apr;29(4):642-8. doi: 10.3174/ajnr.A0918. Epub 2008 Jan 17. PMID: 18202234; PMCID: PMC7978179.

22. Merletti R, Hermens H. Detection and conditioning of the surface EMG signal. In: Merletti, R., Parker, P.A. (Eds.), Electromyography: Physiology, Engineering and Noninvasive Applications. IEEE Press and John Wiley & Sons, Hoboken. 2004; pp. 107-131.

23. Merletti, R., Botter, A. and Barone, U. Detection and Conditioning of Surface EMG Signals. In Surface Electromyography : Physiology, Engineering, and Applications (eds R. Merletti and D. Farina). IEEE Press and John Wiley & Sons, Hoboken. 2016; pp. 1-37.

24. Michieli M (2020). Protocollo per studio esplorativo "Valutazione biomeccanica e metabolica pre e post vertebroplastica in pazienti affetti da mieloma multiplo con crolli vertebrali". Centro di Riferimento Oncologico di Aviano.

25. Norman-Gerum V, McPhee J. Comprehensive description of sit-to-stand motions using force and angle data. J Biomech. 2020 Nov 9;112:110046. doi: 10.1016/j.jbiomech.2020.110046. Epub 2020 Sep 19. PMID: 33099236.

26. Ranavolo A (2021). Principi di elettromiografia di superficie. Dal potenziale d'azione alle applicazioni nei diversi settori della medicina e dell'ingegneria. Edizioni Universitarie Romane

27. Ranavolo A, Mari S, Conte C, Serrao M, Silvetti A, Iavicoli S, Draicchio F. A new muscle co-activation index for biomechanical load evaluation in work activities. Ergonomics. 2015;58(6):966-79. doi: 10.1080/00140139.2014.991764. Epub 2015 Jan 2. PMID: 25555042.

28. Ranavolo A., Varrecchia T., Iavicoli S., Marchesi A., Rinaldi M., Serrao M., Conforto S., Cesarelli M., Draicchio F. Surface electromyography for risk assessment in work activities designed using the "revised NIOSH lifting equation" *Int. J. Ind. Ergon.* 2018;**68**:34–45. doi: 10.1016/j.ergon.2018.06.003.

29. Redfern M, Hughes R, Chaffin D. High-pass filtering to remove electrocardiographic interference from torso EMG recordings. Clin Biomech (Bristol, Avon). 1993 Jan;8(1):44-8. doi: 10.1016/S0268-0033(05)80009-9. Epub 2005 Nov 21. PMID: 23915829.

30. Rosner B, Glynn RJ, Lee ML. The Wilcoxon signed rank test for paired comparisons of clustered data. Biometrics. 2006 Mar;62(1):185-92. doi: 10.1111/j.1541-0420.2005.00389.x. PMID: 16542245.

31. Rudolph KS, Axe MJ, Snyder-Mackler L. Dynamic stability after ACL injury: who can hop? Knee Surg Sports Traumatol Arthrosc. 2000;8(5):262-9. doi: 10.1007/s001670000130. PMID: 11061293.

32. Sandrini S, Dattola R, Smania. Compendio di Neuroriabilitazione. Seconda Edizione Aggiornata ed Ampliata. Session VI, chapter 47–Analisi strumentale, tecniche e tecnologie innovative in neuroriabilitazione. Analisi quantitativa del cammino e nuove tecnologie in riabilitazione neurologica Serrao M, Bartolo M, Ranavolo A, Pierelli F. Verduci Editore, 2020

33. Serrao M, Chini G, Iosa M, Casali C, Morone G, Conte C, et al. Harmony as a convergence attractor that minimizes the energy expenditure and variability in physiological gait and the loss of harmony in cerebellar ataxia. Clin Biomechanics (Bristol, Avon). Elservier ;2017

34. Shaheen NA, Alqahtani M, Alawbthani NS, Thomas A, Alaskar A. Chemotherapy-Induced Peripheral Neuropathy and its Impact on Health-Related Quality of Life among Multiple Myeloma Patients: A Single-Center Experience. Indian J Palliat Care. 2020 Oct-Dec;26(4):506-511. doi: 10.4103/IJPC.IJPC_233_19. Epub 2020 Nov 19. PMID: 33623313; PMCID: PMC7888416.

35. Sharma, A., Sackett, M., Bueddefeld, D., Lambert, P., Wadhwa, V., Kotb, R., & Ahmed, N. (2017). Spinal Involvement in Myeloma: Incidence, Survival and Impact of Radiotherapy. *Cureus Journal of Medical Science*.v

36. Sundjaja JH, Shrestha R, Krishan K. McNemar And Mann-Whitney U Tests. 2022 Jul 18. In: StatPearls [Internet]. Treasure Island (FL): StatPearls Publishing; 2022 Jan–. PMID: 32809534.

37. Tatarelli A, Serrao M, Varrecchia T, Fiori L, Draicchio F, Silvetti A, Conforto S, De Marchis C, Ranavolo A. Global Muscle Coactivation of the Sound Limb in Gait of People with Transfemoral and Transtibial Amputation. Sensors

(Basel). 2020 Apr 29;20(9):2543. doi: 10.3390/s20092543. PMID: 32365715; PMCID: PMC7249183.

38. Tosi P. Diagnosis and treatment of bone disease in multiple myeloma: spotlight on spinal involvement. Scientifica (Cairo). 2013;2013:104546. doi: 10.1155/2013/104546. Epub 2013 Dec 8. PMID: 24381787; PMCID: PMC3870870.

39. Trube N, Riedel W, Boljen M. How muscle stiffness affects human body model behavior. Biomed Eng Online. 2021 Jun 2;20(1):53. doi: 10.1186/s12938-021-00876-6. PMID: 34078371; PMCID: PMC8170985.

40. Varrecchia T, Conforto S, De Nunzio AM, Draicchio F, Falla D, Ranavolo A. Trunk Muscle Coactivation in People with and without Low Back Pain during Fatiguing Frequency-Dependent Lifting Activities. Sensors (Basel). 2022 Feb 12;22(4):1417. doi: 10.3390/s22041417. PMID: 35214319; PMCID: PMC8874369.

41. Varrecchia T, Rinaldi M, Serrao M, Draicchio F, Conte C, Conforto S, Schmid M, Ranavolo A (2018). Global lower limb muscle coactivation during walking at different speeds: Relationship between spatio-temporal, kinematic, kinetic, and energetic parameters. Journal of Electromyography and Kinesiology. 43. 10.1016/j.jelekin.2018.09.012.

42. Wickstroem LA, Carreon L, Lund T, Abildgaard N, Lorenzen MD, Andersen MØ. Vertebroplasty in patients with multiple myeloma with vertebral compression fractures: protocol for a single-blind randomised controlled trial. BMJ Open. 2021 Sep 6;11(9):e045854. doi: 10.1136/bmjopen-2020-045854. PMID: 34489267; PMCID: PMC8422322.

43. Wong WY, Wong MS, Lo KH. Clinical applications of sensors for human posture and movement analysis: a review. Prosthet Orthot Int. 2007 Mar;31(1):62-75. doi: 10.1080/03093640600983949. PMID: 17365886.